

**Electrocatalytic hydrogenation of benzoic acids in a proton-exchange membrane reactor**

Journal:	<i>Organic & Biomolecular Chemistry</i>
Manuscript ID	OB-COM-06-2021-001197.R1
Article Type:	Communication
Date Submitted by the Author:	26-Jul-2021
Complete List of Authors:	Fukazawa, Atsushi; Yokohama National University, Graduate School of Science and Engineering Shimizu, Yugo; Yokohama National University, Graduate School of Science and Engineering Shida, Naoki; Yokohama National University, Graduate School of Science and Engineering Atobe, Mahito; Yokohama National University, Graduate School of Science and Engineering

COMMUNICATION

Electrocatalytic hydrogenation of benzoic acids in a proton-exchange membrane reactor†

Atsushi Fukazawa, Yugo Shimizu, Naoki Shida* and Mahito Atobe*

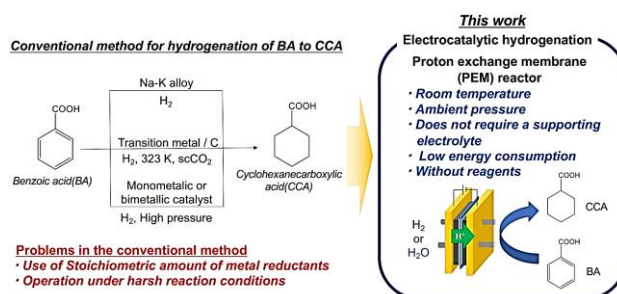
Received 00th January 20xx,
Accepted 00th January 20xx

DOI: 10.1039/x0xx00000x

The highly efficient chemoselective electrocatalytic hydrogenation of benzoic acids (BAs) to cyclohexanecarboxylic acids (CCAs) was carried out in a proton-exchange membrane reactor under mild conditions without hydrogenation of the carboxyl group. Among the investigated catalysts, the PtRu alloy catalyst was found to be the most suitable for achieving high current efficiencies for production of CCAs. An electrochemical spillover mechanism on the PtRu alloy catalyst was also proposed.

The chemoselective hydrogenation of benzoic acids (BAs) to cyclohexanecarboxylic acids (CCAs) has attracted intensive attention because CCAs are important organic intermediates for pharmaceuticals and other useful materials such as praziquantel, caprolactam, and ansatrienin.¹ Great effort has been devoted to finding a suitable method for the efficient and highly chemoselective hydrogenation of BAs to CCAs. Gaude *et al.* have reported the chemoselective hydrogenation of BA and its derivatives without hydrogenation of their carboxyl group by using Na–K alloy reductants (Scheme 1).² However, this method requires handling stoichiometric amounts of metal reductants. To explore a more environmentally friendly chemical process, the chemoselective catalytic hydrogenation of BAs has been carried out with special catalysts based on various noble metals and their alloys.³ However, most of these processes have been conducted under harsh reaction conditions (high pressures and/or high temperatures) because of the need to overcome the high aromatic-ring resonance energy. The harsh reaction conditions may lead not only to hydrogenation of the aromatic ring but also to hydrogenation of the carboxyl group.⁴ Therefore, the development of a chemoselective hydrogenation system that can convert BAs to CCAs under mild conditions is an important research target.

Graduate School of Science and Engineering, Yokohama National University, 79-5 Tokiwadai, Hodogaya-ku, Yokohama, 240-8501, Japan.
E-mail: shida-naoki-gz@ynu.ac.jp (NS), atobe@ynu.ac.jp (MA)
†Electronic Supplementary Information (ESI) available. See DOI: 10.1039/x0xx00000x



Scheme 1. Various methods for the hydrogenation of BA to CCA.

Electrochemical hydrogenation has been demonstrated as an alternative method to chemical hydrogenation because it is performed under benign conditions (room temperature and ambient pressure) without a metal reductant or special catalyst.⁵ However, the conventional electrochemical method has some drawbacks. One major drawback is the addition of a supporting electrolyte, which causes separation problems in the reaction-mixture workup and generates additional waste.⁶ To overcome these problems, we focused on a proton exchange membrane (PEM) reactor.⁷ The PEM reactor was originally developed for fuel cell technologies. As shown in Figure S1 in the ESI, a membrane electrode assembly (MEA) is integrated into the central part of the reactor. The MEA comprises an ion-exchange membrane (i.e., a proton-conducting polymer) sandwiched between a pair of catalyst layers on the anode and cathode sides and performs dual roles as an electrode and a supporting electrolyte. Consequently, the substrate solution does not require a supporting electrolyte. Moreover, the cell resistance can be minimized, enabling the electrochemical reaction to be carried out with less energy consumption than with conventional methods.⁸ In our previous works, we demonstrated the aromatic-ring hydrogenation of toluene,⁹ the semihydrogenation of alkynes to alkenes,¹⁰ and the asymmetric hydrogenation of α,β -unsaturated carboxylic acids using a PEM reactor.¹¹

Herein, we report the chemoselective electrocatalytic hydrogenation of BAs to CCAs in a PEM reactor under mild conditions without adding a supporting electrolyte. Factors such as the current density and the catalyst material were optimized to

establish a highly efficient and chemoselective hydrogenation system. Moreover, in this communication, we proposed a hydrogenation mechanism on cathode catalysts.

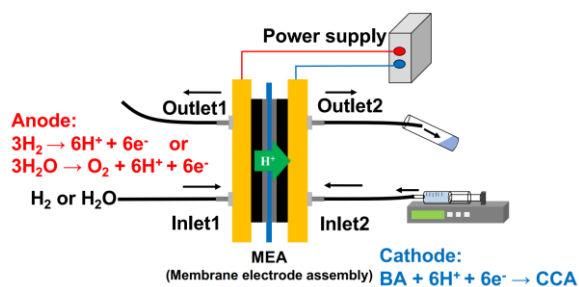


Figure 1. Schematic of a PEM reactor.

We first carried out the hydrogenation of BA (**1a**) to CCA (**2a**) as a model reaction via galvanostatic electrocatalytic hydrogenation in a PEM reactor. To conduct the electrocatalytic hydrogenation in a PEM reactor, humidified H₂ gas was introduced into the anodic chamber (flow rate: 50 mL min⁻¹) and was electrocatalytically oxidized at the Pt anode catalyst to produce protons, as shown in Figure 1. The produced protons were subsequently transported into the cathodic chamber through the proton-conductive polymer and then reduced to a monoatomic hydrogen species (H_{ad}) on the cathode catalyst surface. The H_{ad} species reacted with BA to give CCA. In this case, the anodic reaction is H₂ oxidation, the potential of which is approximately the same as that of the reversible hydrogen electrode (RHE). Therefore, the anode functions not only as the counter electrode but also as a RHE reference electrode,^{8a} and the cathode potential can be monitored during the galvanostatic electrolysis. During the electrocatalytic hydrogenation, a 1,4-dioxane solution including **1a** was introduced to the cathodic chamber by a syringe pump. The hydrogenated products were analysed by gas chromatography (GC). In this work, 1,4-dioxane was selected as a solvent for the electrocatalytic hydrogenation because of its good solubilization of the substrate.

First, the electrocatalytic hydrogenation of **1a** was carried out in a PEM reactor with various noble-metal catalysts (Figure 2). Because Pt₁Ru_{1.5} was found to be a better catalyst material than individual metals such as Pt and Ru for the aromatic-ring hydrogenation of toluene in our previous work,⁹ Pt₁Ru_{1.5} (molar ratio Pt : Ru = 1 : 1.5) as well as single metals such as Pt, Ru, and Rh were used as catalyst samples for the hydrogenation of **1a**. The temporal cathode potential change in the electrocatalytic hydrogenation of **1a** in a PEM reactor is also shown in Figure 2b. Electrocatalytic hydrogenation at 1.5 mA cm⁻² gave the desired product **2a** in excellent current efficiencies (C.E.s) in the case of the Pt₁Ru_{1.5}, Pt, and Rh catalysts, whereas the Ru catalyst exhibited substantially lower activity toward the desired hydrogenation (Figure 2a). In particular, at a current density of 1.5 mA cm⁻², the Pt₁Ru_{1.5} catalyst led to the highest C.E. (99%).

In addition, the hydrogenation of **1a** with the Pt₁Ru_{1.5} catalyst proceeded efficiently at a lower overpotential than was achieved with the other catalysts, indicating better electrocatalytic ability of the Pt₁Ru_{1.5} catalyst (see Figure 2b). None of the catalysts led to hydrogenation of the carboxyl group; the aromatic ring was

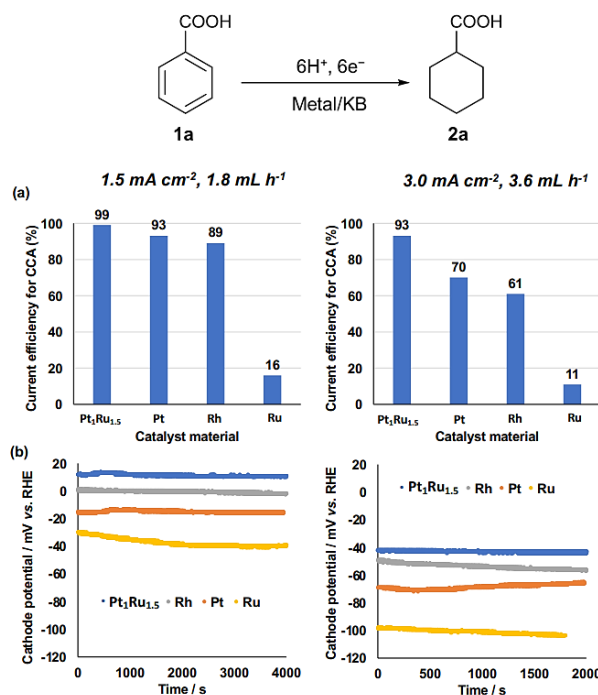


Figure 2. Electrocatalytic hydrogenation of BA (**1a**) to CCA (**2a**) in a PEM reactor. (a) Current efficiency for **2a** and (b) the temporal cathode potential change during electrocatalytic hydrogenation. Experimental conditions: anode catalyst, Pt (loading amount, 0.5 mg cm⁻²); cathode catalyst (loading amount, 0.5 mg cm⁻²); support material of catalysts, Ketjenblack EC300J; cell temperature, r.t.; concentration, 1 M in dioxane; coulomb number, 24 C; flow rate of H₂, 50 mL min⁻¹. The potential values were corrected for the IR drop determined by an impedance measurement. Current efficiency was determined by GC (see ESI).

selectively hydrogenated. As previously mentioned, the carboxyl group in **1a** was also hydrogenated under high-temperature and high-pressure conditions.⁴ However, in the electrocatalytic hydrogenation in a PEM reactor, the aromatic ring could be selectively hydrogenated because the reaction was carried out under mild conditions.

With regard to the current density, the C.E. decreased at 3.0 mA cm⁻² for all of the catalysts. This decrease is attributable to the H₂ evolution reaction (HER) via the coupling of monoatomic H species becoming active because of the greater cathode polarization (see Figure 2b). We also confirmed that no organic products were detected other than **2a**, indicating that H₂ evolution was mainly occurring as a side cathodic reaction. Notably, the Pt₁Ru_{1.5} catalyst showed a high C.E. for the production of **2a** (93%) even at 3.0 mA cm⁻².

In the next stage of our investigation, we carried out X-ray photoelectron spectroscopy (XPS) measurements to confirm the alloying of Pt and Ru in the Pt₁Ru_{1.5} catalyst used in the present work (Figure 3). Figure 3a shows XPS spectra of the Pt 4f region of the Pt and Pt₁Ru_{1.5} catalysts, and Figure 3b shows the XPS spectra of the Ru 3p_{3/2} region of the Ru and Pt₁Ru_{1.5} catalysts. The Pt 4f peak was slightly shifted to the lower-energy side in the spectrum of the Pt₁Ru_{1.5} catalyst (Pt 4f_{7/2}: 72.17 eV, Pt 4f_{5/2}: 75.41 eV) compared with the corresponding peak in the spectrum of the Pt catalyst (Pt 4f_{7/2}: 72.34 eV, Pt 4f_{5/2}: 75.49 eV). By

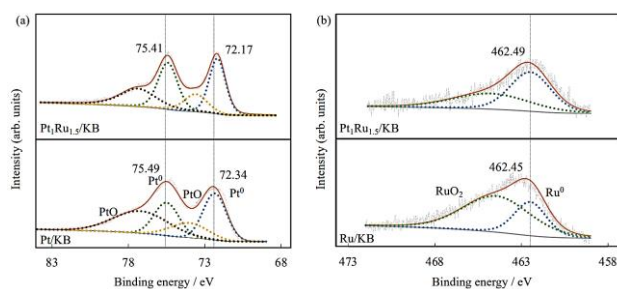


Figure 3. The (a) Pt 4f and (b) Ru 3p_{3/2} regions of the XPS spectra of the Pt, Ru, and Pt₁Ru_{1.5} catalysts.

contrast, the Ru 3p_{3/2} peak was slightly shifted to the higher-energy side in the spectrum of the Pt₁Ru_{1.5} catalyst (Ru 3p_{3/2}: 462.49 eV) compared with the corresponding peak in the spectrum of the Ru catalyst (Ru 3p_{3/2}: 462.45 eV). These shifts are clearly attributable to electron transfer from Ru to Pt in the Pt₁Ru_{1.5} catalyst and to Pt and Ru interacting with each other to form an alloy.

To confirm the effect of alloying on the reactivity, we also carried out the electrocatalytic hydrogenation of **1a** using a catalyst mixed physically with single metals such as Pt and Ru (mixed molar ratio Pt : Ru = 1 : 1.5). However, the C.E. for the production of **2a** was much lower with the physically mixed catalyst (C.E., 67%; 1.5 mA cm⁻², 1.8 mL h⁻¹) than with the Pt₁Ru_{1.5} alloy catalyst. These results indicate that the close proximity of Pt and Ru metals to each other in the alloy is important for achieving efficient hydrogenation reactions.

In our previous work, we demonstrated the aromatic-ring hydrogenation of toluene in a PEM reactor with various cathode catalysts.⁹ In the present investigation, among the tested catalysts, Pt₁Ru_{1.5} exhibited the highest electrocatalytic activity for the aromatic-ring hydrogenation of toluene. In addition, we concluded that the spillover mechanism in which the abundant H_{ad} spillover from the Pt to the Ru in the presence of strongly adsorbed toluene is a key factor for the efficient aromatic hydrogenation of toluene.^{9b} Yamanaka et al.^{8b} have proposed a similar electrochemical spillover mechanism for a RuIr alloy catalyst. The aromatic-ring hydrogenation of **1a** to **2a** can likewise be speculated to also proceed efficiently via the electrochemical spillover mechanism on our PtRu alloy catalyst,

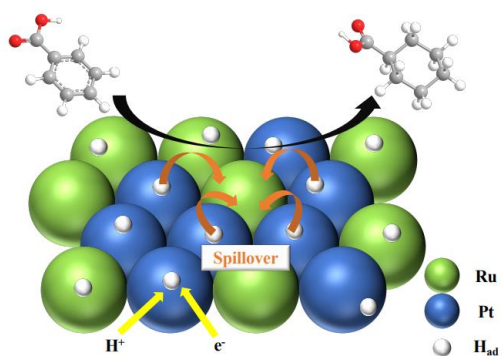


Figure 4. Proposed mechanism for the electrocatalytic hydrogenation of BA using a PtRu catalyst in a PEM reactor.

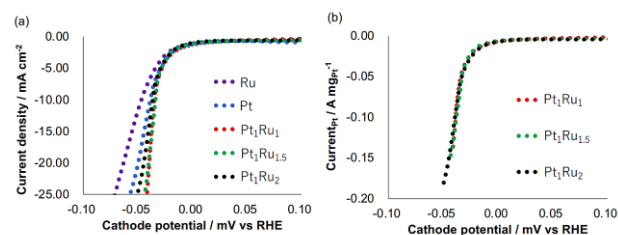


Figure 5. Linear-sweep voltammograms in 1,4-dioxane at Pt, Ru, and PtRu cathode catalysts. Currents are normalized by (a) geometric area and (b) mass loading of Pt. Support material of catalysts, Ketjenblack EC300J; scan rate, 1 mV s⁻¹; cell temperature, r.t.; flow rate of 1,4-dioxane, 1.8 mL h⁻¹; flow rate of H₂, 50 mL min⁻¹. The potential values were corrected for the IR drop determined from an impedance measurement.

as shown in Figure 4. To experimentally verify this assumption, we recorded linear-sweep voltammograms for the HER and estimated the turnover frequency (TOF) for the catalytic hydrogenation of BA using various noble-metal catalysts.

Figure 5a shows linear sweep voltammograms normalized by the geometric area of the electrode. Compared with the other metal catalysts, the Ru catalyst exhibited a greater overpotential for the HER. However, the Pt₁Ru₁, Pt₁Ru_{1.5}, and Pt₁Ru₂ alloy catalysts exhibited lower overpotentials than the Pt single-metal catalyst. Nash et al. have reported that PtRu catalysts exhibit improved HER activity because of the electronic interaction of Ru with Pt and the tuning of the H binding energy.¹² As we also observed in the XPS spectra (Figure 3), Pt atoms of the PtRu alloy were negatively charged by the neighbouring Ru atoms. Therefore, such an electronic interaction of PtRu catalysts is assumed to have improved the HER activity, as shown in Figure 5a.

Figure 5b shows linear-sweep voltammograms for Pt₁Ru₁, Pt₁Ru_{1.5}, and Pt₁Ru₂ alloy electrocatalysts, normalized by the mass loading of Pt (Current_{Pt}). The Current_{Pt} values of the Pt₁Ru₁, Pt₁Ru_{1.5}, and Pt₁Ru₂ catalysts were approximately the same, indicating that the HER proceeded on the Pt site of the PtRu alloy catalysts. Yamanaka et al.^{8b} have reported that the HER activity should be closely related to the aromatic-ring hydrogenation activity because the overpotentials for both the aromatic-ring hydrogenation and the HER are determined by the overpotential for H_{ad} formation. Therefore, the PtRu catalyst gave better C.E.s than the other investigated electrocatalysts (Figure 2a).

Next, to obtain information about the synergy of Pt and Ru in the electrocatalytic hydrogenation of **1a** to **2a**, the catalytic hydrogenation activities of Pt₁Ru₁, Pt₁Ru_{1.5}, and Pt₁Ru₂ alloy electrocatalysts were evaluated at 298 K under a H₂ atmosphere and the TOF normalized by the whole amount of Ru in the catalyst (App-TOF(Ru)) was calculated using Eq. 1 (Table 1):

$$\text{App-TOF(Ru)} = -r(\text{H}_2) \times \frac{a_{\text{wRu}}}{m_{\text{catalyst}} \times \text{wt}_{\text{Ru}}/100} \quad (1)$$

where r is the reaction rate of H₂ (mol h⁻¹), a_{wRu} is the atomic weight of Ru (101.07 g mol⁻¹), m_{catalyst} is the amount of catalyst (5.0 mg), and wt_{Ru} is the mass loading of Ru in the catalyst. As shown in Table 1, the App-TOF(Ru) values for the various PtRu

Table 1. TOF normalized by the whole amount of Ru in PtRu alloy catalysts (App-TOF(Ru)) used in the hydrogenation of **1a**^a

Entry	Catalyst	App-TOF(Ru) ^b / h ⁻¹
1	Pt ₁ Ru ₁	45
2	Pt ₁ Ru _{1.5}	46
3	Pt ₁ Ru ₂	47

^aExperimental conditions: catalyst, 5 mg; temperature, r.t.; concentration, 1 M in dioxane; reaction time, 2 h; ^bApp-TOF(Ru) was determined by GC (see ESI).

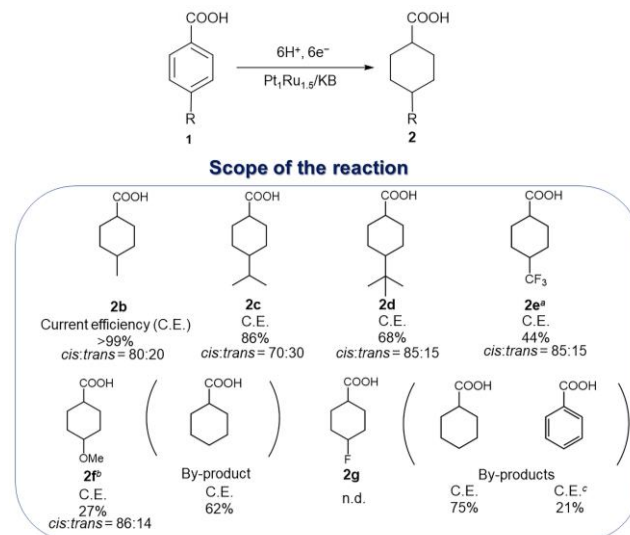
catalysts were approximately the same as each other. This result indicates that catalytic hydrogenation proceeded on the Ru surface of the Pt₁Ru₁, Pt₁Ru_{1.5}, and Pt₁Ru₂ catalysts. However, Tang et al.¹³ estimated the strength of adsorption of **1a** on metal catalysts using first-principles calculations and clarified that the adsorption strength of aromatics on Ru is stronger than that on Pt.

The aforementioned results and discussion strongly support the electrochemical spillover mechanism on the PtRu alloy catalyst in Figure 4 for the efficient electrocatalytic hydrogenation. Thus, protons transported into the cathodic chamber from the anodic chamber through the proton-conductive polymer were reduced to monatomic H species (H_{ad}) adsorbed onto the Pt site in the PtRu alloy catalyst; the H_{ad} then migrated from the Pt surface to the Ru surface, where it finally reacted with **1a** to give **2a**.

In the next section, to demonstrate the general applicability of this hydrogenation system, we carried out the electrocatalytic hydrogenation of various 4-substituted BA derivatives using a PEM reactor and a Pt₁Ru_{1.5} electrocatalyst (Scheme 2). The aromatic-ring hydrogenation of all of the tested BA derivatives proceeded without hydrogenation of their carboxyl group in this system. With regard to stereoselectivity, the corresponding *cis*-isomers were obtained with greater than 70% selectivities. *cis*-Isomers are known to usually be less thermodynamically stable than *trans*-isomers because of steric hindrance. However, in general, *cis*-isomers are mainly obtained via the *syn*-addition of H atoms in the catalytic hydrogenation of 1,4-disubstituted arenes using solid metal catalysts.¹⁴ Therefore, the hydrogenation of 4-substituted BA derivatives with H_{ad} on cathode catalysts in a PEM reactor might proceed in a similar manner as ordinary catalytic hydrogenation with solid metal catalysts.

The size of the alkyl substituents influenced the C.E.; that is, the efficiency decreased with increasing substituent size of the substrates (**1b–d**). This result might be due to the fact that larger substituents impede the ability of the reacting substrate to access the catalyst surface. In addition, in the case of the alkyl-substituted BAs, no other organic products formed via side reactions, indicating that H₂ evolution was likely the main side reaction. However, we found that the *cis* selectivity was also influenced by the metal catalyst. The order of *cis* selectivity was Rh > PtRu > Pt for all of the 4-alkyl substituted BAs (Table S1). This result likely reflects the adsorption strength of the aromatic rings on the respective catalyst surfaces.

The introduction of an electron-withdrawing group onto the benzene ring of the substrate acid (**1e**) resulted in a decrease in the C.E. In general, a decrease in electron density of the benzene



Scheme 2. Electrocatalytic hydrogenation of 4-substituted BA derivatives. Experimental conditions: anode catalyst, Pt (loading amount, 0.5 mg cm⁻²); cathode catalyst, PtRu (loading amount, 0.5 mg cm⁻²); support material of catalysts, Ketjenblack EC300J; cell temperature, r.t.; coulomb number, 24 C; concentration of BAs, 1 M; flow rate of H₂, 50 mL min⁻¹. Current efficiency (C.E.) and *cis/trans* selectivity were determined by GC (see ESI). ^aConcentration, 0.5 M. ^bConcentration, 0.1 M. ^cC.E. for benzoic acid was determined by HPLC (see ESI).

ring due to the introduction of an electron-withdrawing group improves the reactivity of reduction processes such as hydrogenation; this result therefore differs from the general case. The substrate **1e** with a relatively bulky functional group such as trifluoromethyl group is also reasonably expected to have limited access to the catalyst. When the substrate acid **1f** with an electron-donating group such as a methoxy group was subjected to the hydrogenation process, the methoxy group was eliminated via a side reaction, resulting in CCA as the sole product. Wijaya et al. have reported that the elimination of a methoxy group proceeds via a two-electron reduction in the electrocatalytic hydrogenation of guaiacol ($E_{0\text{ red}} = 0.38\text{ V}$ vs standard hydrogen electrode (SHE)).¹⁵ Hence, a similar elimination of the methoxy group might proceed in this case. The electrocatalytic hydrogenation was also carried out with 4-fluorobenzoic acid **1g**. However, a chemoselective aromatic-ring hydrogenation did not occur; defluorination mainly occurred in this case. That is, both BA and CCA were obtained as hydrogenated products.

The effect of current density on the C.E. and *cis/trans* ratio was also investigated in the electrocatalytic hydrogenation of alkyl-substituted BAs. The stereoselectivity did not change at any current density (1.5–12 mA cm⁻²) for any of the three acids; however, the C.E. decreased with increasing current density because of the concomitant H₂ evolution (Tables S2–S4).

In the aforementioned hydrogenations, a hydrogen oxidation reaction was used as the anodic process. However, the use of H₂ gas may be a disadvantage for practical applications of this method. In principle, the use of H₂ gas is not a problem as long as the anodic process of the PEM reactor is a proton-providing reaction. Among candidate anodic reactions, water oxidation (H₂O → 2H⁺ + 1/2O₂ + 2e⁻) is the most ideal process from the

perspective of operating costs, safety, and green methodology. Hence, we carried out the electrocatalytic hydrogenation of **1a** in combination with the anodic oxidation of water. The electrocatalytic hydrogenation was performed galvanostatically at 1.5 mA cm⁻² and gave the desired product **2a** with a good C.E. (75%). In addition, the temporal voltage change was also stable during the galvanostatic hydrogenation of **1a** in a PEM reactor (Figure S17). Thus, the PEM reactor system could provide the desired hydrogenated product even without H₂ gas, making it safe and compact compared with conventional hydrogenation systems.

Conclusions

In summary, we demonstrated the highly efficient chemoselective hydrogenation of BAs to CCAs in a PEM reactor under mild conditions without hydrogenation of the carboxyl group. Among the tested catalysts, PtRu exhibited the best performance as a cathode catalyst material for electrocatalytic hydrogenation in a PEM reactor. Linear-sweep voltammetry measurements and estimations of App-TOF(Ru) clarified that the spillover mechanism, in which abundant H_{ad} species spillover from the Pt part to the Ru part in the presence of strongly adsorbed BA, is a key factor for the efficient aromatic hydrogenation of BA to CCA. From the generality experiments with 4-substituted BA derivatives, we found that the corresponding *cis*-isomers were obtained with greater than 70% selectivities. In addition, we confirmed that the steric rather than the electronic factors of the substrate acids are responsible for the reactivity of the electrolytic aromatic-ring hydrogenation. Furthermore, the electrocatalytic aromatic-ring hydrogenation of BA could be carried out in combination with the anodic oxidation of water. The proposed system is safe and compact compared with conventional hydrogenation systems. Therefore, we are currently preparing a much larger PEM reactor in order to achieve the gram-scale synthesis.

Conflicts of interest

There are no conflicts to declare.

Acknowledgements

This work was financially supported by JST CREST Grant No. JP65R1204400, Japan.

References

- (a) A. D. Dwivedi, R. K. Rai, K. Gupta and S. K. Singh, *ChemCatChem*, 2017, **9**, 1930–1938; (b) W. Lian, B. Chen, B. Xu, S. Zhang, Z. Wan, D. Zhao, N. Zhang, and C. Chen, *Ind. Eng. Chem. Res.*, 2019, **58**, 2846–2856; (c) B. S. Moore, H. Cho, R. Casati, E. Kennedy, K. A. Reynolds, J. M. Beale, U. Mocek and H. G. Floss, *J. Am. Chem. Soc.*, 1993, **115**, 5254–5266; (d) H. Shinkai, M. Nishikawa, Y. Sato, K. Toi, I. Kumashiro, Y. Seto, M. Fukuma, K. Dan and S. Toyoshima, *J. Med. Chem.*, 1989, **32**, 1436–1441; (e) H. Shinkai, K. Toi, I. Kumashiro, Y. Seto, M. Fukuma, K. Dan, and S. Toyoshima, *J. Med. Chem.*, 1988, **31**, 2092–2097.
- D. Gaude, R. Legoaller, J.L. Luche and J.L. Pierre, *Tetrahedron Lett.*, 1984, **25**, 5897–5898.
- (a) X. Xu, M.H. Tang, M.X. Li, F. Xu, H.R. Li and Y. Wang, *ACS Catal.* 2014, **4**, 3132–3135; (b) J.A. Anderson, F.–M. McKenna, A. Linares–Solano and R.P.K. Wells, *Catal Lett*, 2007, **119**, 16–20; (c) C.H. Yen, H.W. Lin and C.S. Tan, *Catalysis Today*, 2011, **174**, 121–126; (d) M. Tang, S. Mao, M. Li, Z. Wei, F. Xu, H. Li and Y. Wang, *ACS Catal.* 2015, **5**, 3100–3107; (e) H. Jiang, X. Yu, R. Nie, X. Lu, D. Zhou and Q. Xia, *Appl. Catal. A*, 2016, **520**, 73–81; (f) R. Nie, H. Jiang, X. Lu, D. Zhou and Q. Xia, *Catal. Sci. Technol.*, 2016, **6**, 1913–1920; (g) Z. Jiang, G. Lan, X. Liu, H. Tang and Y. Li, *Catal. Sci. Technol.*, 2016, **6**, 7259–7266; (h) X.H. Lu, Y. Shen, J. He, R. Jing, P.P. Tao, A. Hu, R.F. Nie, D. Zhou and Q.H. Xia, *Mol. Catal. Commun.* 2012, **17**, 29–33; (i) H. Wang and F. Zhao, *Int. J. Mol. Sci.*, 2007, **8**, 628–634.
- (a) H. Wang and F. Zhao, *Int. J. Mol. Sci.*, 2007, **8**, 628–634; (b) R.L. Augustine, *Catal. Rev. Sci. Eng.*, 1976, **13**, 285–316; (c) X. Xu, M.H. Tang, M.X. Li, F. Xu, H.R. Li and Y. Wang, *ACS Catal.*, 2014, **4**, 3132–3135.
- (a) M.J. Torres, P. Sánchez, A. de Lucas-Consuegra and A. Raquel de la Osa, *Molecular Catalysis*, 2020, **492**, 110936–110945; (b) M. Yan, Y. Kawamata and P.S. Baran, *Chem. Rev.* 2017, **117**, 13230–13319; (c) J.–I. Yoshida, A. Shimizu and R. Hayashi, *Chem. Rev.* 2018, **118**, 4702–4730; (d) T. Fuchigami and T. Tajima, *Electrochemistry*, 2006, **74**, 585–589; (e) M. Yan, Y. Kawamata and P.S. Baran, *Angew. Chem., Int. Ed.*, 2018, **57**, 4149–4155.
- (a) D. Horii, M. Atobe, T. Fuchigami and F. Marken, *Electrochem. Commun.*, 2005, **7**, 35–39; (b) K. Otsuka and I. Yamanaka, *Appl. Catal.*, 1986, **26**, 401–404.
- (a) Z. Ogumi, K. Nishio and S. Yoshizawa, *Electrochim. Acta.*, 1981, **26**, 1779–1782; (b) E. Raoult, J. Sarrazin, A. Tallec, *J. Appl. Electrochem.*, 1984, **14**, 639–643; (c) J.Jörissen, *Electrochim. Acta*, 1996, **41**, 553–562.
- (a) S. Mitsushima, Y. Takakuwa, K. Nagasawa, Y. Sawaguchi, Y. Kohno, K. Matsuzawa, Z. Awaludin, A. Kato and Y. Nishiki, *Electrocatalysis*, 2016, **7**, 127–131; (b) Y. Inami, H. Ogiwara, S. Nagamatsu, K. Asakura and I. Yamanaka, *ACS Catal.*, 2019, **9**, 2448–2457; (c) K. Matsuoka, K. Miyoshi, Y. Sato, *J. Power Sources*, 2017, **343**, 156–160; (d) T. Fukushima and M. Yamauchi, *Chem. Commun.*, 2019, **55**, 14721–14724.
- (a) K. Takano, H. Tateno, Y. Matsumura, A. Fukazawa, T. Kashiwagi, K. Nakabayashi, K. Nagasawa, S. Mitsushima and M. Atobe, *Bull. Chem. Soc. Jpn.*, 2016, **89**, 1178–1183; (b) A. Fukazawa, K. Takano, Y. Matsumura, K. Nagasawa, S. Mitsushima and M. Atobe, *Bull. Chem. Soc. Jpn.*, 2018, **91**, 897–899.
- (a) A. Fukazawa, J. Minoshima, K. Tanaka, Y. Hashimoto, Y. Kobori, Y. Sato, M. Atobe, *ACS Sustainable Chem. Eng.* 2019, **7**, 11050–11055; (b) S. Nogami, K. Nagasawa, A. Fukazawa, K. Tanaka, S. Mitsushima, M. Atobe, *J. Electrochem. Soc.*, 2020, **167**, 155506–155512.
- A. Fukazawa, K. Tanaka, Y. Hashimoto, Y. Sato, M. Atobe, *Electrochem. Commun.*, 2020, **115**, 106734–106738.
- J. Nash, J. Zheng, Y. Wang, B. Xu, Y. Yan, *J. Electrochem. Soc.*, 2018, **165**, J3378–J3383.
- M. H. Tang, S. J. Mao, X. F. Li, C. H. Chen, M. M. Li, and Y. Wang, *Green Chem.* 2017, **19**, 1766–1774.
- (a) W. Kitching, H.A. Olszowy, G.M. Drew, W. Adcock, *J. Org. Chem.*, 1982, **47**, 5153–5156; (b) V. Mévellec, A. Roucoux, E. Ramirez, K. Philippot, B. Chaudret, *Adv. Synth. Catal.*, 2004, **346**, 72–76.
- Y. P. Wijaya, T. G. Neuhaeusler, R. D. D. Putra, K. J. Smith, C. S. Kim, E. L. Gyenge, *ChemSusChem*, 2020, **13**, 629–639.